Journal of Molecular Liquids 266 (2018) 770–780

Contents lists available at ScienceDirect

Journal of Molecular Liquids

journal homepage: www.elsevier.com/locate/molliq

Synergistic effect of the sequential intercalation of three types of surfactants in the exfoliation degree of bentonite clay in films of cassava☆

Mayra Kerolly Sales Monteiro [a], Victor Rafael Leal de Oliveira [b,*], Francisco Klebson Gomes dos Santos [b], Eduardo Lins de Barros Neto [a], Ricardo Henrique de Lima Leite [b], Edna Maria Mendes Aroucha [b], Karyn Nathallye de Oliveira Silva [a]

[a] Universidade Federal do Rio Grande do Norte/UFRN, 59.078-970, RN, Brazil
[b] Universidade Federal Rural do Semi-Árido/UFERSA, 59.600-000, RN, Brazil

ARTICLE INFO

Article history:
Received 5 February 2018
Received in revised form 14 June 2018
Accepted 3 July 2018
Available online 4 July 2018

Keywords:
Biodegradable film
Nanocomposite
Physicochemical properties
Modified clay
Surfactants

ABSTRACT

A method of obtaining exfoliated nanocomposite films based on biopolymers has been reported. The method is based on the incorporation of modified bentonite clay by mixing surfactants into a biodegradable matrix. The biopolymer used was cassava starch, which has a high hydrophilicity, which makes it less desirable than synthetic polymers, when used as a film matrix for coating. The improvement of this was proposed with the formation of a nanocomposite matrix by the high exfoliation of the modified bentonite clay used as reinforcement material. The degree of exfoliation of the sequential modification in bentonite with three surfactants throughout the cassava starch film was investigated by XRD, FTIR, AFM, SEM, OM and contact angle. The physicochemical properties of the nanocomposite films were analyzed for water vapor permeability, ductility, opacity, thermal stability and water solubility. Finally, the clay modified in the presence of the three surfactants was the reinforcement material that contributed the most to the physical/chemical properties of the control starch film, among which it reduced 90.6% of the water vapor permeability, as well as 77.43% of the maximum dissolution.

1. Introduction

The use of biopolymer films in the food industry as packaging for coating of fruit and vegetable is increasing due to the intense demand for good products [1,2]. This occurs from biopolymers being biodegradable matrices from renewable sources that can reduce environmental pollution caused by non-degradable synthetic polymer residues [3]. To compete with these conventional materials, biopolymers must have their physicochemical properties modified, since their hydrophilic nature influences the barrier properties of the coating [4]. Therefore, the demand for an edible coating that is sustainable and with excellent water vapor barrier, mechanical, optical and thermal properties is a challenge.

Cassava starch, cheap and affordable product, is considered to be one of the most promising candidate materials for the manufacture of biodegradable films [5]. However, low thermal, optical, mechanical and water vapor barrier properties limit the starch-based films to be used [6]. An option to improve these properties is the incorporation of clay minerals as reinforcing material to the biopolymer matrix forming bionanocomposites [7,8].

In this perspective, bionanocomposite films have improved physicochemical properties in relation to the original biofilm, considering that nanomaterials are scattered to the biopolymer matrix giving it a barrier character [6]. However, the simple mixing of biopolymer and clay minerals does not always result in the generation of a bionanocomposite, since the degree of dispersion of the clay minerals in the biopolymer matrix is directly related to obtaining a film with uniform properties. This difficulty is due to the weak interactions between the biopolymer and the natural clay, resulting in an intercalated dispersion of the reinforcing material in the biopolymer matrix [9,10].

The solution of this, in turn, is for the natural clay to present counterions on the intercalated surface of the silicate layers, which favors the ion exchange reaction with modifiers through hydrogen bonds [11]. Such modifiers provide space and compatibility for the biopolymer structure to interlace and thus exfoliate the silicate layers of the clay by dispersing them uniformly forming bionanocomposites [7,8]. In fact, in previous studies [12–15] was observed improvements in physical and chemical properties of the cassava starch film due to the formation of bionanocomposites by the presence of bentonite clay modified by ionic surfactants.

Finally, the present work aimed to apply a new reinforcement material in cassava starch films aiming a potential improvement of the physical/chemical properties of the pure starch film, such material is bentonite clay synergistically modified by three types of surfactants

☆ The article was accepted for publication under the special issue on Polymers in Solution and in Liquids - 14th Brazilian Polymer Congress.

* Corresponding author.
E-mail address: vrafaeloliveira@uol.com.br (V.R.L. de Oliveira).

https://doi.org/10.1016/j.molliq.2018.07.012
0167-7322/

(cationic, anionic and nonionic). The performance of this was compared to that of bentonite clay in its natural state and also modified with both (cationic and anionic) and with a (cationic) type of surfactant.

2. Materials and methods

2.1. Materials

Cassava starch was supplied by the Indústria Primícias do Brasil, Macaíba, RN, Brazil. The clay used was Calcium Bentonite (Bent-Ca), gently supplied by Armil Mineraçãodo Nordeste (AMN), Parelhas, RN, Brazil, with a mean particle size of 0.074 mm and a cation exchange capacity of 90 mmol/100 g (determined by the method of adsorption of methylene blue). The chemical composition of Bent-Ca used was characterized by X-ray fluorescence (XRF) and the result is listed in Table 1. The cationic surfactant used was cetyltrimethyl ammonium bromide (CTAB) of molecular formula $C_{19}H_{42}BrN$, supplied by Proquímios. The anionic surfactant was sodium dodecyl sulfate (SDS) of molecular formula $NaC_{12}H_{25}SO_4$, supplied by Oxitene. The nonionic surfactant was the class of lauryl alcohol (ALEOn) with an ethoxylation number equal to 23, termed as diethylene glycol monododecyl ether ($C_{16}H_{34}O_3$), supplied by Oxitene. The plasticizer used was glycerol, with the denomination of glycerin P.A. - ACS with molecular formula $C_3H_5(OH)_3$.

2.2. Surface clay modification

Three surface modifications in Bent-Ca were prepared, respectively, in the presence of CTAB (1.0 CTC), CTAB (1.0 CTC) + SDS (0.2 CTC) and CTAB (1.0 CTC) + SDS (0.2 CTC) + ALEO (0.2 CTC) and named: OBent-I, OBent-II and OBent-III. Each superficial chemical modification in the bentonite clay was determined by the methodology proposed by Liao et al. [16], where the mass of each surfactant in 100 mL of distilled water was established for each modification in relation to the Bent-Ca ion exchange capacity.

The dispersion of the bentonite was 6% (by weight) in each system. For this, 6 g of bentonite and 94 g of distilled water were mixed and stirred for 30 min at 80 °C in a thermostat. The previous procedure was continued for a further 2 h after addition of the surfactant solutions, and a thermostatic bath was subsequently used to disperse the particles in the mixture. Finally, each mixture was filtered and washed to remove excess salt. The material trapped in the filtration was brought to the oven at 60 °C and held for 24 h. After drying, they were macerated with mortar and pistil, and then sieved in ABNT No. 200 sieve (φ = 0.074 mm).

2.3. Obtaining the films

The film was prepared according to the methodology proposed by Cyras et al. [17] and Monteiro et al. [13]. Five solutions were prepared containing each 70 ml of distilled water, 5 g of cassava starch and 30% (w/w) of glycerol in relation to the starch mass. The solutions were heated at 70 °C for 15 min until complete homogenization.

In parallel, four distinct mixtures of 30 mL were prepared, containing distilled water, respectively: Bent-Ca, OBent-I, OBent-II and OBent-III. The mixtures were placed in an ultrasonic bath at room temperature, 25 °C. The amount of clay is related to 5% in dry mass of biopolymer.

The starch solutions and the respective clay mixtures were homogenized forming four filmogenic solutions. To obtain the control film the step of the addition of clay was neglected, being this filmogenic solution constituted only of starch, glycerol and distilled water. The five final film-forming solutions were placed in an ultrasonic bath for 30 min to facilitate dissolution.

Each formed solution was used for the casting of films, where 40 ml of film-forming solution were poured onto a plastic plate with a radius of 7.5 cm. Plates were maintained at 25 °C for 36 h, after drying each film was demolded by the end of the respective plate, with the aid of a stainless steel forceps of thin and anti-magnetic tip. The five films obtained following the described procedure were denominated as: Control (starch + glycerol + water), FB (starch + glycerol + Bent-Ca + water), FOBI (starch + glycerol + OBent-I + glycerol), FOBII (starch + glycerol + OBent-II + water) and FOBIII (starch + glycerol + OBent-III + water).

2.4. Characterization of films

2.4.1. X-ray diffraction – XRD

The XRD analyzes were performed on a Bruker D2 Phaser diffractometer using Cu-Kα radiation (λ = 1.5406 Å) with Ni filter and LYNXEYE detector. The scanning rate was 0.01°/s for a 2θ interval of 2° to 30° with a current of 10 mA and a voltage of 30 kV. The obtained diffractograms were compared with the JCPDS (Joint Committee on Powder Diffraction Standards). Using HighScore Plus Version 3.0e. Rietveld's refinement of the diffraction data was employed using the Maud software (version 2.55).

2.4.2. Fourier transform by infrared radiation – FTIR

The infrared absorption spectra were obtained with a BRUKER spectrometer, model FT-IR VERTEX 70, with scanning of 4000 to 400 cm^{-1}, resolution of 4 cm^{-1} and number of scans 16. The samples were characterized directly by total reflectance attenuated, without any preparation.

2.4.3. Scanning electron microscopy – SEM

The micrographs were performed in microscope bench of brand HITACHI model TM 3000 top, with detector High-sensitivity semiconductor back scattered electron detector, with magnification of 1 kx operating at 15 kV voltage acceleration with tungsten filament. The powder of the samples was added in aluminum stubs and analyzed.

2.4.4. Atomic force microscopy – AFM

The morphological surface of the films was analyzed using a Shimadzu atomic force microscope, Model SPM-9700. The analysis was performed in the tapping mode with a scanning speed of 1 Hz. No treatment was done on the sample for analysis.

2.4.5. Optical microscopy – OM

Optical microscopy observations were performed using an Olympus BX52 microscope, equipped with an Olympus C5050Z camera. Optical micrographs were obtained for each film using the incident light mode. The samples were carefully poured into an alumina carrier and spread under glass cover, at room temperature, before observations.

2.4.6. Contact angle – CA

The contact angle measurements are based on the sessile drop technique, according to Boinovich et al. [18]. The apparatus is composed of a mobile base with sample holder, a camera (VP 540 s, Intelbras) and a light source. The angle calculation methodology was based on the images formed by the intersection of the liquid-solid. The software used to calculate the contact angle was Surftens 4.5.

Table 1
Chemical composition of Bent-Ca.

	Elements	SiO_2	Al_2O_3	Fe_2O_3	CaO	MgO	K_2O	Na_2O	Others
Mass (%)	Bent-Ca	53.8943	15.7085	12.1755	10.1266	2.8674	1.6885	0.4705	3.0687

2.5. Analysis of the physicochemical properties of the films

2.5.1. Thickness

The thickness of the films was measured using a Mitutoyo micrometer (Model MDC-25M, MFG/Japan). The measurements were taken at five random points throughout the film.

2.5.2. Water vapor permeability – WVP

The water vapor permeability rate of the films was determined gravimetrically, according to the standard method ASTM E96–93 [19] with slight modification adopted in the studies of Oliveira et al. [20]. The films were cut into square pieces (2 cm × 2 cm) and sequentially deposited on top of the WVP measuring cells. The water level was up to 1 cm below the film. The weight of each cell was measured before being deposited in a desiccator which contained silica stones at the bottom, as well as a relative humidity of 50% and internal temperature of 29 °C. Cell weight was measured every hour over a period of 8 h. The WVP of the films was calculated in g/m·s·Pa as follows:

$$WVP = \frac{W \cdot L}{A \cdot t \cdot \Delta P} \quad (1)$$

where:

W: Weight of the water permeated through the film (g);
L: Film thickness (m);
A: Permeation area (m^2);
t: Permeation time (s);
ΔP: Pressure difference to water vapor between the two sides of the film (Pa).

2.5.3. Solubility

To collect the solubility data, was used the methodology adapted from Rhim et al. [21]. With this, discs with 2 cm of diameter were dried at 105 °C for 1 h. The disks were immersed in distilled water at room temperature, shaken for 24 h. Then the discs were again dried at 105 °C for 1 h. The solubility can be calculated from Eq. (2):

$$S = \frac{mi - mf}{mi} \times 100 \quad (2)$$

where

mi: initial mass (g)
mf: final mass (g).

2.5.4. Opacity

The opacity of the films was determined by the colorimeter (CR 10, Minolta), calibrated with a standard white background and a standard black background. The opacity values were calculated according to Eq. (3), according to Fakhouri et al. [22]:

$$Op = \frac{Op_N}{Op_B} \times 100 \quad (3)$$

where:

O_{pN}: opacity of the film against a black background
O_{pB}: Opacity of the film against a white background.

2.5.5. Mechanical testing

The mechanical properties of the films were determined using a DL5000/10,000 Series EMIC 23 Series, EMIC (Paraná, Brazil) Testing Machine which operates according to the standard method of ASTM D882–12 [23] at an assay speed of 5 mm/min with total force application of 5 kN. The samples follow the same standard and are evaluated with length of 50 mm, width of 5 mm and obeying the maximum thickness of 0.25 mm.

2.5.6. Thermogravimetric analyzes – TGA

A thermogravimetric analyzer and simultaneous calorimeter, model TG209F1 Libra and manufacturer NETZSCH were used for the analysis. All the tests were carried out obeying the following parameters: alumina crucible; nitrogen purge gas; bleed gas flow rate of 50 mL/min; heating rate of 10 °C/min; final temperature of 600 °C and sample mass of 5 mg.

2.5.7. Statistical analysis

All qualitative analysis data were collected in triplicate. The significant difference between means was established by the Duncan method with a level of statistical significance lower than 5%.

3. Results and discussion

3.1. Characterization of films as intercalated or exfoliated nanocomposites

3.1.1. X-ray diffraction

Fig. 1 shows the overlap of the XRD patterns of the control film, FB, FOBI, FOBII, FOBIII, and Bent-Ca and OBent-III.

Fig. 1a shows the typical XRD patterns of cassava starch that according to Zhu [6] characterize in 2θ between 2 and 30° its semicrystalline structure whose diffraction tendencies dominate in the amorphous region. It is possible to notice that the films FB, FOBI, FOBII, and FOBIII tend to characterize bionanocomposites, due to the peak corresponding to 001 plane of Bent-Ca clay to appear at angles of <2°. Moreover, the characteristic peaks evidenced in the investigated scanning range were 2θ = 23°, 20°, 19° and 16°, respectively, with reference to the presence of the silicate layers identified in values of diffraction angles lower than Bent-Ca in 2θ = 25° [24,25].

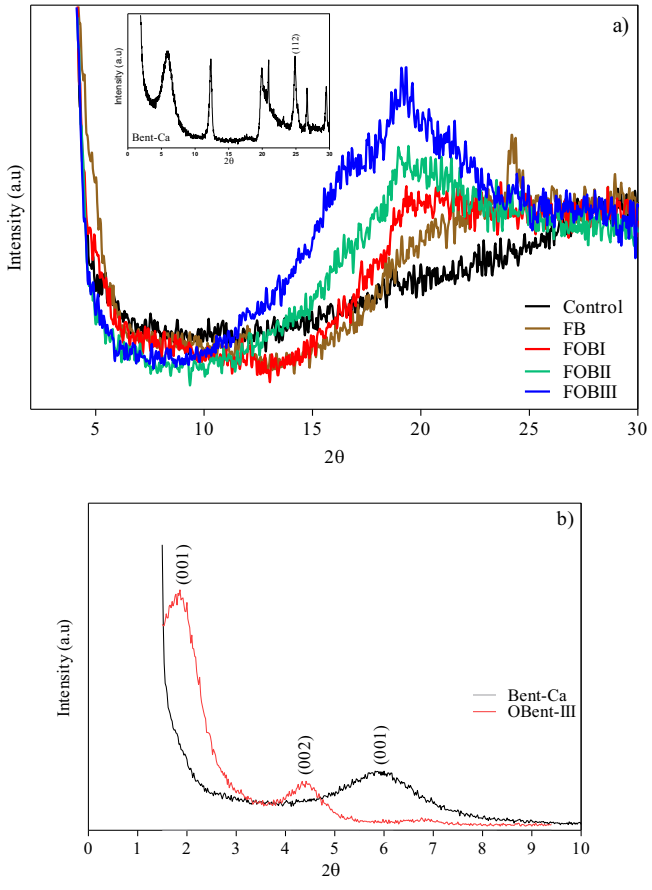

Fig. 1. XRD patterns: a) Control Film, FB, FOBI, FOBII, FOBIII and Bent-Ca and b) Bent-Ca and OBent-III.

Thus, it is verified that the structure of the cassava starch has been able to interlace among the layers of silicate by dispersing them along the biopolymer matrix in the following order FOBIII > FOBII > FOBI > FB. FOBIII showed the highest degree of dispersion of the reinforcing material characterizing the best exfoliated bionanocomposite, according to Chiu et al. [8], it follows from OBent-III to show a high basal space (see Fig. 1b), thus providing space for the starch to interweave between these layers, exfoliating them. This fact also arises from OBent-III to provide electrostatic compatibility through the induced dipole bonds between the monomers of the starch structure and the functional groups of the clay modifier [7,8,26].

This result also characterizes FB as an intercalated bionanocomposite, where according to Romero-Bastida et al. [27] occurs because the thermoplasticized starch with glycerol becomes vulnerable to establish intermolecular hydrogen bonding with the surface of the Bent-Ca, but this presents stacked layers of silicate compactibilizadas by Van der Waals force that makes such connections difficult, thus not having the interaction of the starch with the Bent-Ca sufficient force to disperse the silicate layers, with this, the Bent-Ca aggregation occurs stacked along the starch.

3.1.2. Fourier transform by infrared radiation

The FTIR spectra of the control starch films and in the presence of Bent-Ca and OBent in the range of 4000–2800 cm^{-1} are overlapped on Fig. 2.

Fig. 2 shows the appearance bands referents of stretching of hydrocarbon bonds (—CH), common in the samples at 2900 cm^{-1} [28], as well as the appearance of elongated bands at 3300 cm^{-1}, corresponding to the stretching of bond of free hydroxyl groups (—OH) [29]. However, in this last case it was possible to notice that there was a distinction in the five transmittance bands, which may be associated with the number of hydrogen bonds established in each case. Thus, the greater the elongation of the transmittance band, the greater the number of hydrogen bonds established in the film [30].

The layers forming the stacked structure of the natural clay have a three-dimensional crystalline structure with an octahedral leaf at the center of two tetrahedral leafs. This structure results in the presence of hydroxyl groups on the clay surface, stabilized by the presence of calcium cations in the interlamellar galleries. This fact does not favor the complete aggregation of the clay in the structure of the thermoplastic starch, but it can prove the existence of interaction by the lower presence of free hydroxyl groups in the bands of the FB film in relation to the control starch film [12].

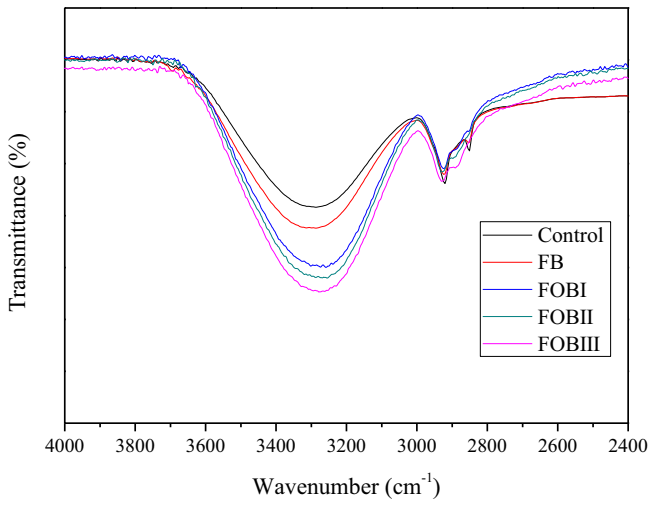

Fig. 2. Overlap of spectra in the infrared region of the starch film of control, FB, FOBI, FOBII and FOBIII.

On the other hand, the FOBIII film had the lowest presence of free hydroxyl groups in relation to the other two films also in the presence of modified clay (FOBI and FOBII), proving that the degree of interaction of the reinforcement material with the structure of cassava starch is directly proportional to the structural characteristics of the modifier, such as molecular weight, concentration and type [7].The sequence of the degree of interaction established between the biopolymer and the reinforcing material was therefore FOBIII > FOBII > FOBI > FB.

3.1.3. Atomic force microscopy

Fig. 3 shows the micrographies of the topographic study done on cassava starch films, where the values of maximum roughness height and average roughness are shown.

The topographic study of control films, FB, FOBI, FOBII and FOBIII, is shown in Fig. 3 (a), (b), (c) and (d), respectively. The mean roughness order was Control > FB > FOBI > FOBII > FOBIII, with the control film of 33.63 nm and FOBIII 6.24 nm. The higher roughness observed in the control film can be explained by the presence of starch and glycerol, by the thermoplasticization, the formation of a biopolymer matrix of high mobility, vulnerable to establishing interaction with the medium, since glycerol is responsible for breaking the inter and intramolecular forces established between amylose and amylopectin constituents of the starch matrix [31].

The lower roughness of the FOBIII can be explained, as observed in the FTIR, by the greater exfoliation of the reinforcing material that evenly interacts with the starch matrix reducing its maximum roughness height. Such interaction is established by dipole bonds induced through the entanglement of OBent-III functional groups and the monomeric structure of the starch.

The roughness of the film FB was lower than the control, corroborating with the intercalation observed in the XRD and interaction in the FTIR, so that it shows the existence of dispersion of the reinforcement material, but in an aggregate form. The values found here corroborate with the results found by Flaker et al. [32] and Qi et al. [33].

3.1.4. Scanning electron microscopy

The SEM analyzes in the control, FB, FOBI, FOBII and FOBIII films are shown in Fig. 4.

Through the SEM Fig. 4(a) and AFM (Fig. 3(a)) it can be seen a disorganized and non-homogeneous thermoplastic film structure. The observed results of the cassava starch have a structure intertwined between the amylose and amylopectin molecules through hydrogen bonds, forming crystalline areas ordered radially. Among these crystalline areas, there are amorphous regions, in which the molecules have no particular orientation. In turn, it is in these crystalline areas that the aggregation of the plasticizer occurs, being responsible for reducing intermolecular forces and increasing the mobility of the biopolymer chain making it disorganized [34].

Fig. 4(b) shows that natural clay formed tactoids along the biopolymer matrix, due to the lack of affinity between the starch and Bent-Ca structure, since there are interlamellar inorganic cations that make Bent-Ca partially electronegative, in which case the silicate layers remain stacked, allowing the formation of gaps along the FB film, forming an intercalated bionanocomposite [21].

Fig. 4 (c), (d) and (e) show that the modified and starch bionanocomposites form a cohesive and homogeneous biopolymer matrix in order FOBIII > FOBII > FOBI, because the clay is in each case organophilized with a modifier compatible with the monomeric structure of the starch, thereby allowing the interlacing thereof through the silicate layers. Thus, the higher the structural characteristics of the modifier the better the dispersion of the clay along the biopolymer matrix characterizing the formation of a bionanocomposite with high exfoliation [35]. The higher homogeneity of the starch film in the presence of OBent-III in relation to the other films, can be evidenced by the lower average roughness observed in the AFM image (see Fig. 3(e)).

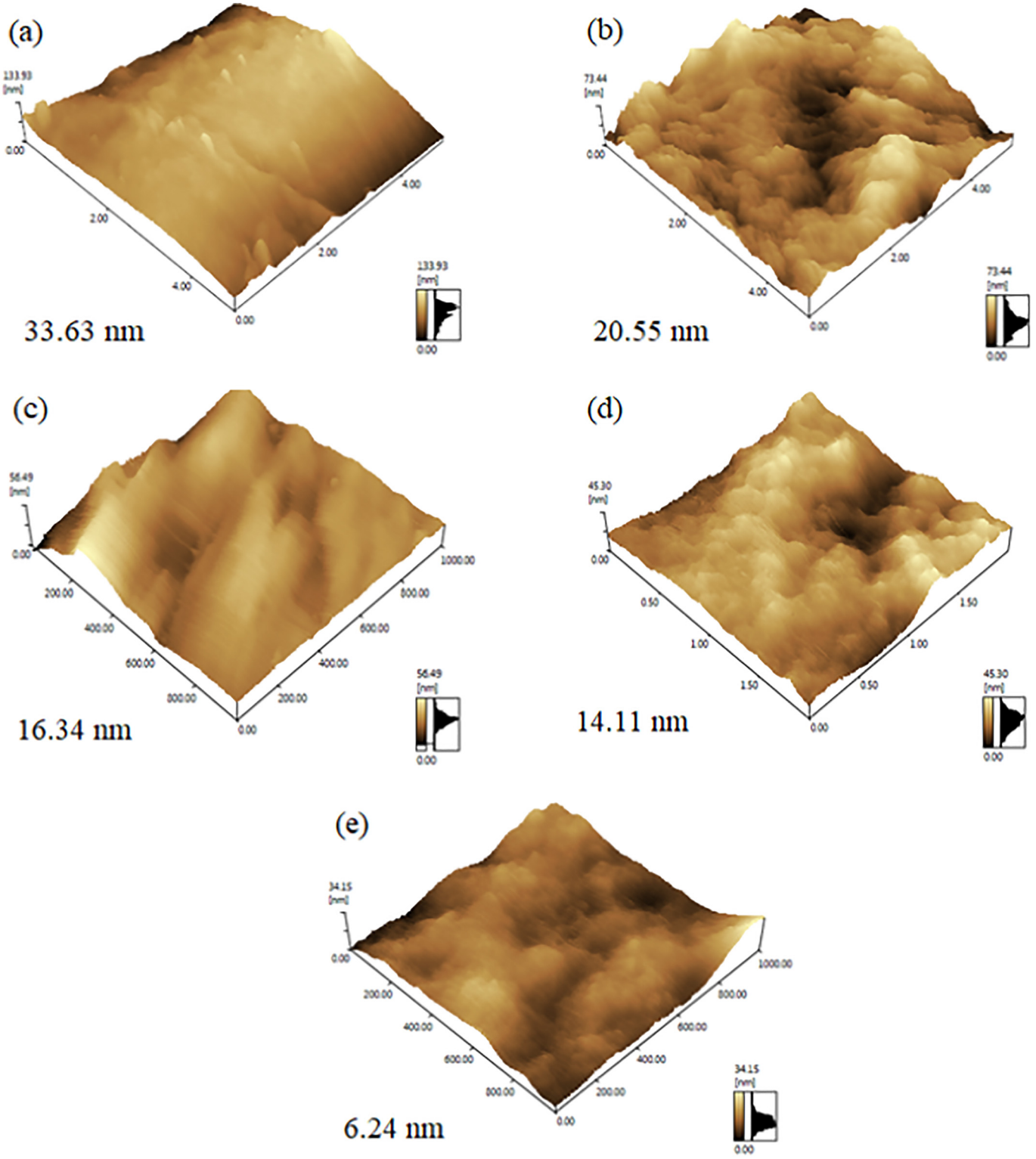

Fig. 3. Atomic force micrographs and mean surface roughness values of the films: (a) Control, (b) FB, (c) FOBI, (d) FOBII and (e) FOBIII. Atomic force micrographs and mean surface roughness values of films. Scale: 5 × 5 [μm].

3.1.5. Optical microscopy

Fig. 5 shows images made on the films in an optical microscope.

Micrographs (Fig. 5(a), 5(b), 5(c), 5(d) and 5(e)) showed a change in the morphology of the surfaces of the films with the reinforcement content. On the one hand, all thermoplastic films presented small crystals in the whole film which, according to Zhu [6], are related to the starch granules formed by amylose and amylopectin. On the other hand, in the micrography of the bionanocomposites was observed the presence of crystals larger than those observed by the starch granules due to the presence of the reinforcing material.

The micrographs evidenced in Fig. 5(a), (b), (c), (d) and (e) showed a change in the morphology of the surfaces of the starch films with the

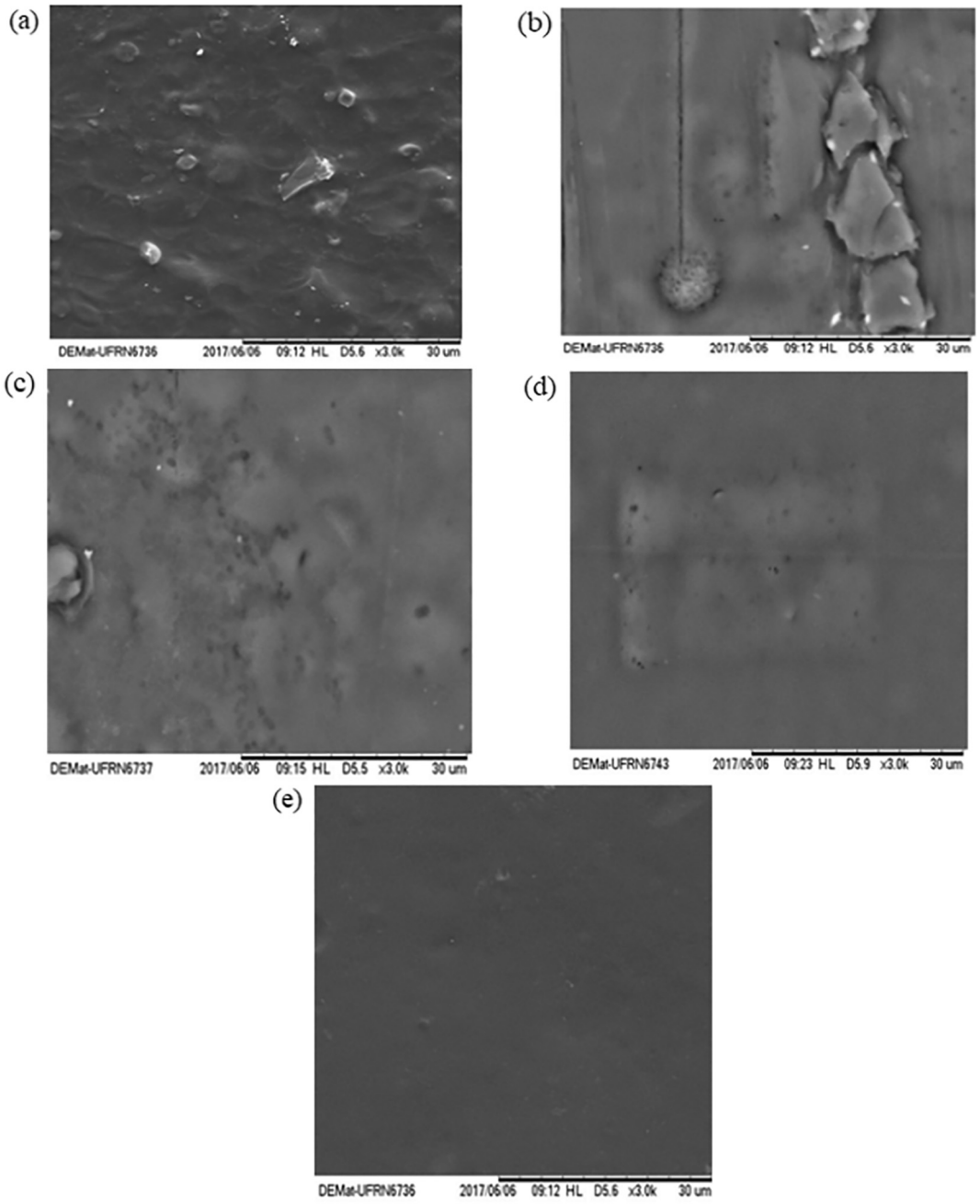

Fig. 4. Scanning electron micrographs of films: (a) Control, (b) FB, (c) FOBI, (d) FOBII and (e) FOBIII. Magnitude: 1 kx.

reinforcement content. On the one hand, all the films presented crystals of small size, which according to Zhu [6] are related to the granules of starch formed by the interlacing of amylose and amylopectin responsible for forming the structure of the starch. On the other hand, in the micrograph of the starch films with clay was observed the presence of crystals larger than the starch granules due to the presence of the reinforcing material [17].

Thus, it was observed in Fig. 5(b) that Bent-Ca disperses non-uniformly, allowing the formation of regions with gaps containing only the starch granules. In Fig. 5(c), (d) and (e), among the modified reinforcement materials, OBent-III was the one with the least exposure of the starch granules, corresponding to the more uniform dispersion of the silicate layers, evidencing the highest degree of exfoliation. These results explain several studies about the physicochemical properties of biodegradable films such as those made by Huskić et al. [36], Shah et al. [37] and Chivrac et al. [38].

3.1.6. Contact angle

Fig. 6 shows the shape of the water droplet on the surface of the control films, FB, FOBI, FOBII and FOBIII.

Fig. 6(a) shows an angle of 36 °C formed between the drop of water and the cassava starch film, evidencing the tendency of the starch to interact in polar medium. This fact had as a parameter of comparison recent works like those of Flaker et al. [32], Saberi et al. [39] and Chen et al. [40], where biopolymer films of low affinity were considered, in medium with difference of humidity, those with angles >65°.

Fig. 6(b) shows that even using Bent-Ca as a reinforcing material, the starch film still interacts with water, considerably, proving that the clay disperses in an aggregate manner leaving the film with gaps. Fig. 6(c), (d) and (e) show an increase in the contact angle, thus demonstrating uniform dispersion of the reinforcing material.

Finally, among the analyzed films, FOBIII was the one that established the lowest interaction with the polar medium, presenting

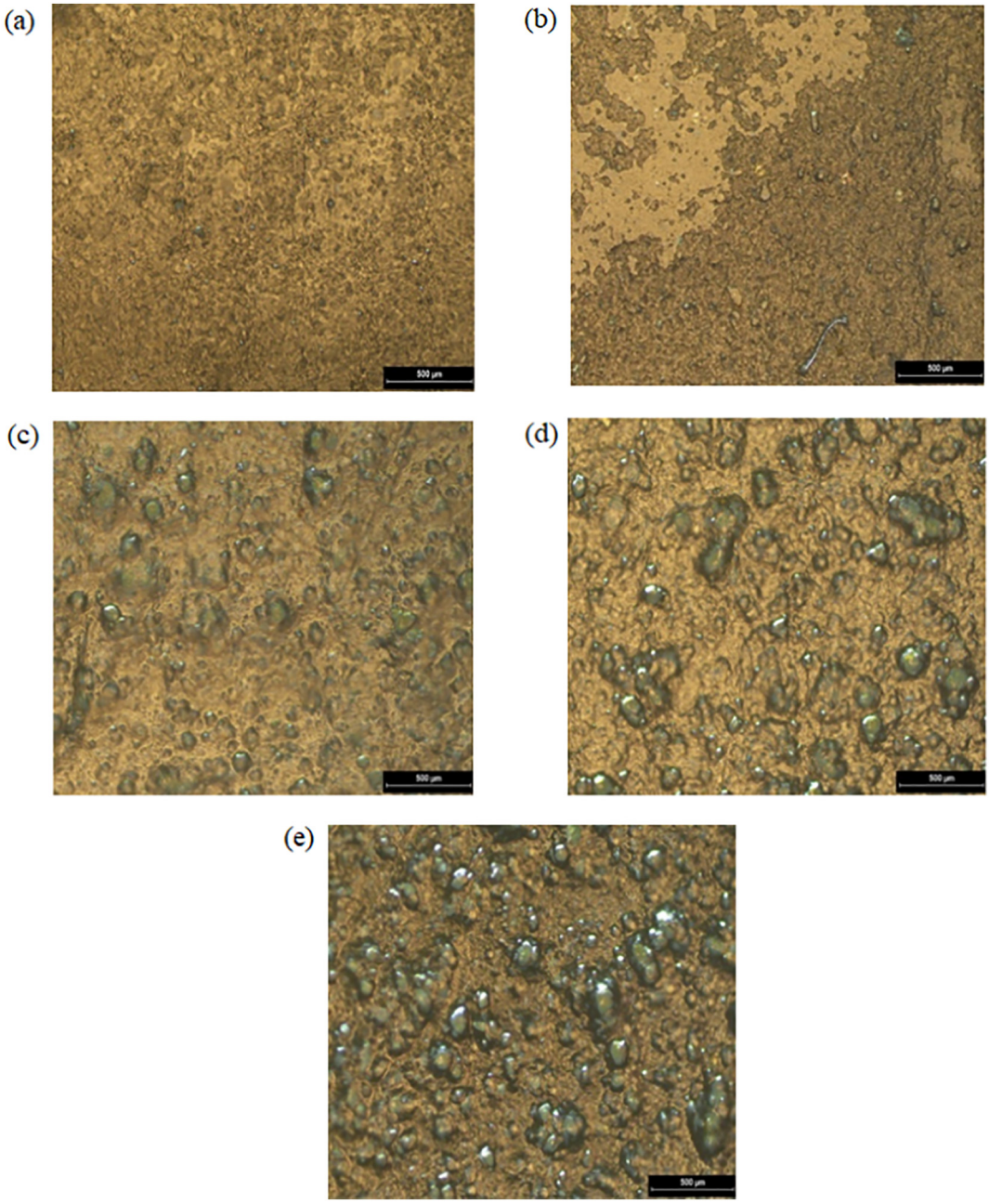

Fig. 5. Optical micrograph of films: (a) Control, (b) FB, (c) FOBI, (d) FOBII and (e) FOBIII. Magnitude: 200×.

an angle of 69.93°. This is due to the electrostatic compatibility between the starch and OBent-III, so that the larger the functional groups of the modifier larger is the space between the silicate layers that the monomeric structure finds to interlace by establishing intermolecular bonding with such functional groups [41]. Therefore, the silicate layers disperse evenly throughout the structure of the starch reducing its ability to carry hydrogen bonds with the medium.

3.2. Analysis of the physicochemical properties of films

3.2.1. Barrier, mechanical and optical properties

Table 2 shows the effects of the Bent-Ca sequential modification on the barrier properties (WVP and Solubility), mechanical (tensile strength and elongation at break) and opacity (opacity) of cassava starch films.

Different letters indicate the statistical difference ($p < 0.05$).

According to Table 2, the WVP values decreased in the order of FOBIII > FOBII > FOBI > FB, the FOBIII film having a 90.6% reduction in relation to the control starch film, because it had a structure almost completely exfoliated, exhibiting the lowest WVP (1.04927×10^{-10} g·m/m^2·s·Pa) among the films analyzed. The exfoliation of OBent-III in the starch matrix significantly increased the effective length of the route for the water molecules to diffuse and cross the film [26]. On the other hand, it can be seen that the increase of WVP of the films in the presence of Bent-Ca was probably due to the discontinuous phase formed between the Bent-Ca structure and the biopolymer matrix, since Bent-Ca has a difference of polarity in relation to the structure of the biopolymer [42]. This fact results in the films with unmodified clay, a weaker electrostatic interconnection that becomes the bionanocomposite with larger numbers of gaps resulting in the increase of the WVP of the films [43].

In Table 2, it was also observed that the modified clays OBent-I, OBent-II and OBent-III gave the starch film a maximum dissolution of around 31%, 25% and 17%, respectively; presenting OBent-III greater

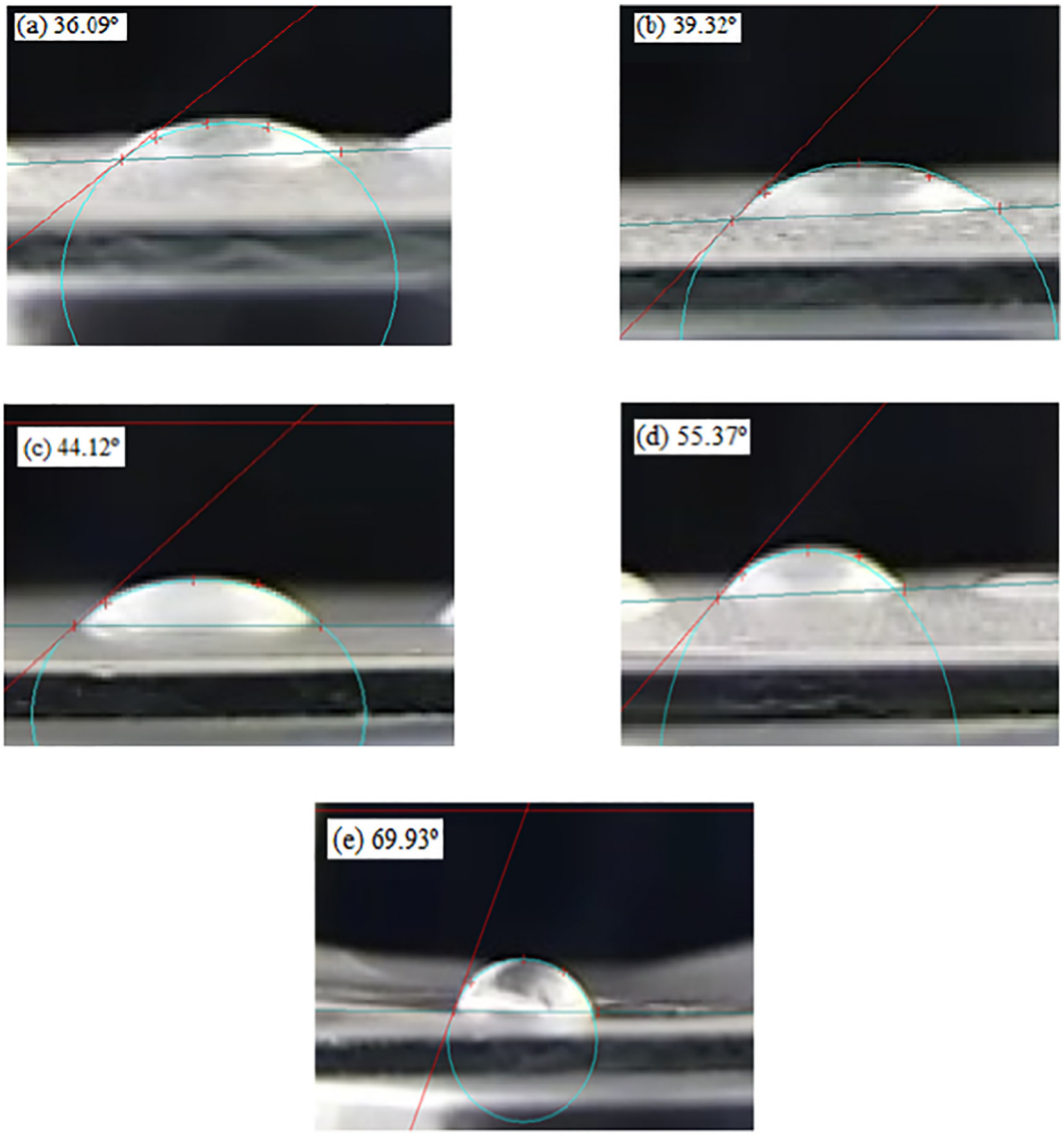

Fig. 6. Images of the drop of water on the surface of the films: A) Control, (b) FB, (c) FOBI, (d) FOBII and (e) FOBIII.

influence on the solubility of the starch film in water. The main reason for this reduction in solubility in relation to the control film (73%) is the presence of the high content of functional groups between the lamellar layers of OBent-III that makes, due to polarity difference, the compatible biopolymer matrix, thus, a strong interaction is obtained by reducing the gaps of the medium and contributing to the barrier formation on the contact surface of the biopolymer. Thus, the crosslink density in the composite films increases along structural characteristics increase of the modifier, resulting in lower solubility values [44,45]. In the Bent-Ca films the maximum dissolution percentage of the film was 64%, higher than that presented in the films with OBent, since the FB presents a film-forming structure of high gaps that contributes to a smaller cross-linking of the composite film and increases its adhesion to water molecules [46].

The light transmission in the starch films decreased with the presence of the reinforcing material as shown in Table 2. The opacity values of the starch and Bent-Ca or OBent composites did not differ significantly from the value presented by the control starch film and may be considered transparent. The starch film showed 43.7% opacity, which increased to 47.4%, 47.6% and 47.9% with the addition of OBent-I, OBent-II and OBent-III, respectively, or 45.5% with the addition of Bent-Ca (see Table 2). The OBent bionanocomposite gave the cassava starch matrix a higher opacity when compared to the starch film with Bent-Ca. This may be due to the fact that the modified clay is dispersed

Table 2
Values of water vapor permeability (WVP), solubility, tensile strength, elongation at break and opacity of cassava starch films.

	WVP ($g \cdot m/m^2 \cdot s \cdot Pa$)		Solubility (%)		Tensile strength (Mpa)		Elongation at break (%)		Opacity (%)	
Control	1.12E−09	7.89E−11^{a}	73.28	0.928^{a}	7.538	0.251^{a}	24.894	0.830^{a}	43.678	0.843^{a}
FB	7.53E−10	5.16E−11^{b}	63.75	0.751^{ab}	11.009	0.367^{b}	31.302	1.043^{b}	45.549	0.382^{ab}
FOBI	3.88E−10	5.08E−11^{c}	30.647	0.380^{c}	16.438	0.548^{c}	36.963	1.232^{c}	47.413	0.238^{ab}
FOBII	2.60E−10	2.18E−11^{c}	25.095	0.391^{c}	18.065	0.602^{c}	43.891	1.463^{d}	47.604	0.591^{b}
FOBIII	1.05E−10	1.16E−11^{c}	16.539	0.359^{c}	20.748	0.692^{c}	52.326	1.744^{e}	47.946	0.532^{b}

throughout the biopolymer matrix uniformly and in a suitable portion (5% of the dry mass of the polymer), but this fact did not significantly influence the visual appearance of the original film [47]. The greater reduction in the light transmission of the FB film in relation to the control suggests that the natural clay was not completely dispersed by forming agglomerations intercalated in the matrix of the biopolymer, preventing the passage of light through the film [48,49].

According to Saurabh et al. [35] the improvement of the mechanical properties of biopolymer films is due to the increase of their flexibility, which in turn is measured by the elongation at break and is defined as the ability of the film to deform before breaking. In fact, the cassava starch films in the presence of OBent presented better flexibility, characterizing them as high ductility materials in relation to the control starch films and in the presence of Bent-Ca. The ductility sequence of the bionanocomposite films was: FOBIII > FOBII > FOBI, where FOBIII showed the maximum elongation at break and tensile strength, around 52.326% and 20.748 MPa (see Table 2), suggesting that the film with the highest exfoliation of reinforcing material resulted in better dispersion of the applied tension, characterizing the obtaining of a more ductile material in relation to the control film and the film in the presence of Bent-Ca. In turn, the starch film with Bent-Ca shows to be more flexible compared to the control starch film (see Table 2) due to the formation of aggregated tactoid in the biopolymer matrix as observed in SEM. Such tactoids can act as a nucleating agent, resisting the elongation of the

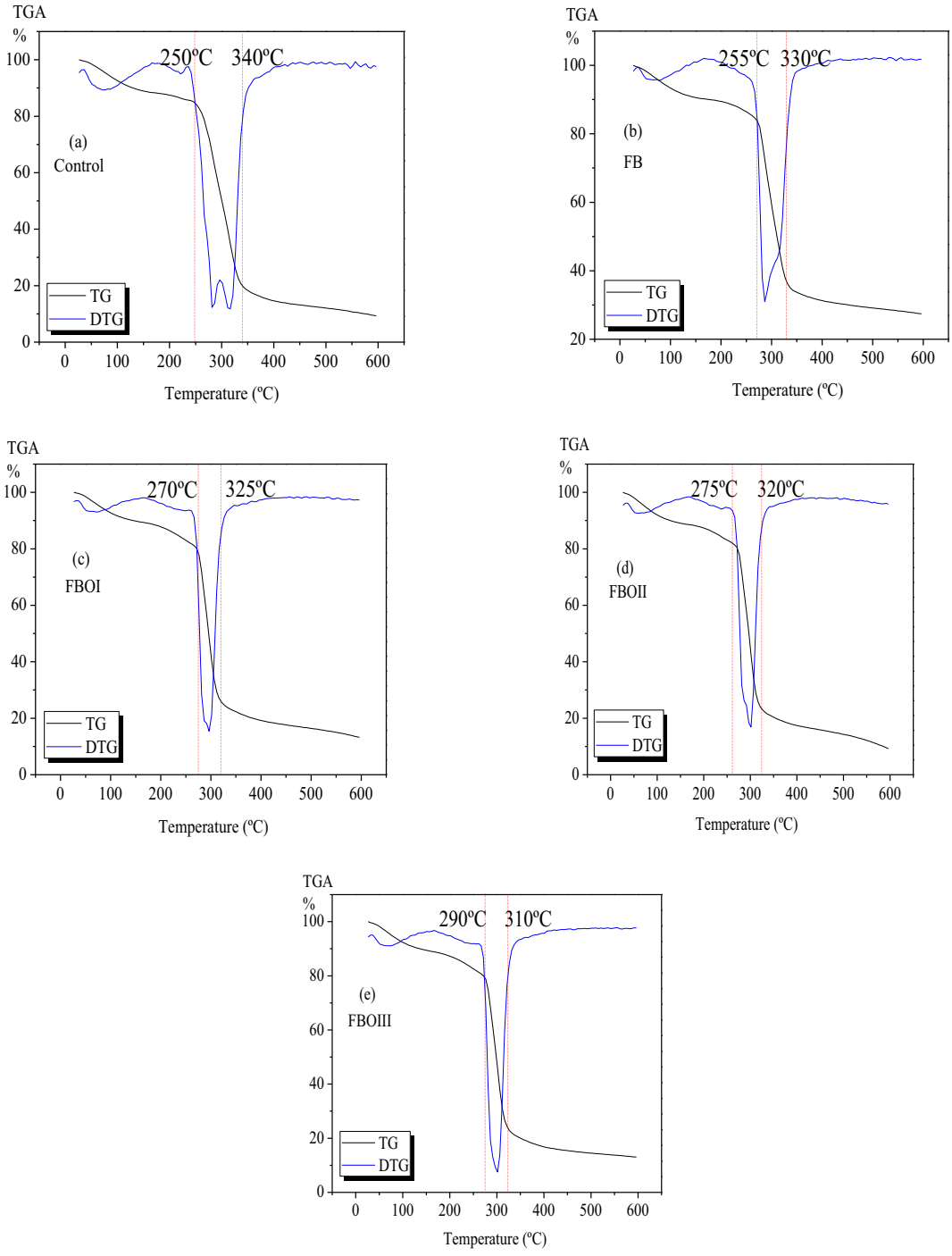

Fig. 7. Thermogravimetric curves of the films: (a) Control, (b) FB, (c) FOBI, (d) FOBII and (e) FOBIII.

main chain interconnected with the biopolymer matrix by hydrogen bonding. The results are as observed by Cyras et al. [15], Romero-Bastida et al. [25] and Matsuda et al. [50].

3.2.2. Thermal property

Fig. 7 shows the behavior of five curves TG/DTG referring to the control films, FB, FOBI, FOBII and FOBIII.

The TG/DTG curves show an initial peak representing the evaporation of the water adsorbed by the starch and the reinforcing material, as well as the evaporation of the glycerol used, together with the evaporation of low molecular weight compounds. Such peak is in the temperature range of 25–250 °C for the control film, between 25 and 255 °C for the FB film, between 25 and 270 °C, 25–275 °C and 25–290 °C for FOBI, FOBII and FOBIII films, respectively (see Fig. 7(a), (b), (c), (d) and (e)). With this, FOBIII was the film that delayed the beginning of the second phase that refers to the decomposition of the starch, around 45 °C in relation to the control film.

In this perspective, the FOBIII film presented the best thermal stability, evidencing the highest peak in a lower temperature range when compared to the other films. This may be due to OBent-III when modified with the presence of a mixture of surfactants, to cause a greater interaction with the biopolymer matrix, as evidenced by the FTIR and AFM analyzes, and therefore to act as a heat barrier to control film when compared to Bent-Ca and OBent I and II. Similar behaviors were observed by Romero-Bastida et al. [25], Gao et al. [26], Qi et al. [33] and Saurabh et al. [35].

4. Conclusion

The improvement of the physical properties of the cassava starch film was obtained with the formation of a bionanocomposite exfoliated in the presence of OBent-III as reinforcing material. The characterization of the FOBIII film evidenced that OBent-III allowed a greater interlacing of the biopolymer matrix between the silicate layers resulting in greater exfoliation among the reinforcement materials investigated. In fact, it was concluded that OBent-III made starch film a material more resistant to rupture; improved its barrier property causing reduction in both WVP and its maximum dissolution capacity in water; further retarded the decomposition point of the starch thus improving the thermal stability of the control film and finally the presence of any reinforcing material investigated did not affect the visual appearance of the control film.

Acknowledgement

To the Conselho Nacional de Desenvolvimento Científico e Tecnológico (CNpq) for financial support; to the laboratories of structural characterization of materials (UFRN), of chemical processes (UFERSA), of mechanical tests (UFERSA), of molecular sieves (UFRN), multifunctional materials and experimentation (UFRN) and the oil and gas education and research center (UFRN).

References

[1] S. Shankar, J.W. Rhim, Bionanocomposite films for food packaging applications, Reference Module in Food Science, 2018.
[2] F. Garavand, M. Rouhi, S.H. Razavi, I. Cacciotti, R. ohammadi, Improving the integrity of natural biopolymer films used in food packaging by crosslinking approach: a review, Int. J. Biol. Macromol. 104 (2017) 687–707.
[3] Z. Fang, Y. Zhao, R.D. Warner, S.K. Johnson, Active and intelligent packaging in meat industry, Trends Food Sci. Technol. 61 (2017) 60–71.
[4] N. Wilton, B.A. Lyon-Marion, R. Kamath, K. Mcvey, K.D. Pennell, A. Robbat JR, Remediation of heavy hydrocarbon impacted soil using biopolymer and polystyrene foam beads, J. Hazard. Mater. 349 (2018) 153–159.
[5] C.M. Leis, A.R. Nogueira, L. Kulay, C.C. Tadini, Environmental and energy analysis of biopolymer film based on cassava starch in Brazil, J. Clean. Prod. 143 (2017) 76–89.
[6] F. Zhu, Composition, structure, physicochemical properties, and modifications of cassava starch, Carbohydr. Polym. 122 (2015) 456–480.
[7] M. Kotal, A.K. Bhowmick, Polymer nanocomposites from modified clays: recent advances and challenges, Prog. Polym. Sci. 51 (2015) 127–187.
[8] C.W. Chiu, T.K. Huangb, Y.C. Wangb, B.G. Alamanib, J.J. Linb, Intercalation strategies in clay/polymer hybrids, Prog. Polym. Sci. 39 (2014) 443–485.
[9] A. Giannakas, A. Patsaoura, N.M. Barkoula, A. Ladavos, A novel solution blending method for using olive oil and corn oil as plasticizers in chitosan based organoclay nanocomposites, Carbohydr. Polym. 157 (2017) 550–557.
[10] R.T. Silva, M.M.M.G.P.G. Mantilaka, S.P. Ratnayake, G.A.J. Amaratunga, K.M. Nalin Silva, Nano-MgO reinforced chitosan nanocomposites for high performance packaging applications with improved mechanical, thermal and barrier properties, Carbohydr. Polym. 157 (2017) 739–747.
[11] D.L. Silva, A.V. Silva, H.S. Ferreira, Study of organic surfactants sorption in bentonite clays, Cerâmica 62 (2016) 294–304.
[12] M.K.S. Monteiro, V.R.L. Oliveira, F.K.G. Santos, R.H.L. Leite, E.M.M. Aroucha, R.R. Silva, Analysis of water barrier, mechanical and thermal properties of nanocomposites based on cassava starch and natural clay or modified by anionic exchange, Materials Research-Iberoamerican Journal of Materials (2017)https://doi.org/10.1590/1980-5373-mr-2016-1087.
[13] M.K.S. Monteiro, V.R.L. Oliveira, F.K.G. Santos, R.H.L. Leite, E.M.M. Aroucha, J.O. Vitoriano, Hydrophilicity, solubility and optical properties in composite films of gelatin and bentonite clay in its natural form or modified, Mater. Sci. Forum 912 (2018) 136–140.
[14] M.K.S. Monteiro, V.R.L. Oliveira, F.K.G. Santos, E.L. Barros Neto, R.H.L. Leite, E.M.M. Aroucha, R.R. Silva, K.N.O. Silva, Incorporation of bentonite clay in cassava starch films for the reduction of water vapor permeability, Food Res. Int. 105 (2018) 637–644.
[15] V.R.L. Oliveira, T.D.N. Xavier, N.O. Araujo, J.G.L. de Almeida, F.K.G. Santos, E.M.M. Aroucha, R.H.L. Leite, Evaluation of biopolymeric films of cassava starch with incorporation of clay modified by ionic exchange and its application as a coating in a fruit, Mater. Res.-Ibero American Journal of Materials (2018)https://doi.org/10.1590/1980-5373-mr-2016-0928.
[16] L. Liao, G. Lv, D. Cai, L. Wu, The sequential intercalation of three types of surfactants into sodium montmorillonite, Appl. Clay Sci. 119 (2016) 82–86.
[17] V.P. Cyras, L.B. Manfredi, T.T. Minh-Tan, A. Vazquez, Physical and mechanical properties of thermoplastic starch/montmorillonite nanocomposite films, Carbohydr. Polym. 73 (2008) 55–63.
[18] L. Boinovich, A.M. Emelyanenko, V.V. Korolev, A.S. Pashinin, Effect of wettability on sessile drop freezing: when superhydrophobicity stimulates an extreme freezing delay, Langmuir 30 (6) (2014) 1659–1668.
[19] ASTM International, ASTM E96/E96M-12, Standard Test Methods for Water Vapour Transmission of Materials, Annual Book of Standards, 1993.
[20] V.R.L. Oliveira, F.K.G. Santos, R.H.L. Leite, E.M.M. Aroucha, K.N.O. Silva, Use of biopolymeric coating hydrophobized with beeswax in post-harvest conservation of guavas, Food Chem. 259 (2018) 55–64.
[21] J.W. Rhim, Effect of PLA lamination on performance characteristics of agar/κ-carrageenan/clay bio-nanocomposite film, Food Res. Int. 51 (2013) 714–722.
[22] F.M. Fakhouri, S.M. Martelli, T. Caon, J.I. Velasco, L.H.I. Mei, Edible films and coatings based on starch/gelatin: film properties and effect of coatings on quality of refrigerated Red Crimson grapes, Postharvest Biol. Technol. 109 (2015) 57–64.
[23] ASTM International, ASTM D882-12, Standard Test Method for Tensile Properties of Thin Plastic Sheeting, ASTM International. Annual Book of Standards, West Conshohocken, 2012.
[24] G. Coativy, N. Gautier, B. Pontoire, A. Buléon, D. Lourdin, E. Leroy, Shape memory starch–clay bionanocomposites, Carbohydr. Polym. 116 (2015) 307–313.
[25] C.A. Romero-Bastida, L.A. Bello-Pérez, G. Velazquez, J. Alvarez-Ramirez, Effect of the addition order and amylose content on mechanical, barrier and structural properties of films made with starch and montmorillonite, Carbohydr. Polym. 127 (2015) 195–201.
[26] Y. Gao, Y. Dai, H. Zhang, E. Diao, H. Hou, H. Dong, Effects of organic modification of montmorillonite on the performance of starch-based nanocomposite films, Appl. Clay Sci. 99 (2014) 201–206.
[27] C.A. Romero-Bastida, D.R. Tapia-Blácido, G. Méndez-Montealvo, G. Velázquez, A. Ramirez, Effect of amylose content and nanoclay incorporation order in physicochemical properties of starch/montmorillonite composites, Carbohydr. Polym. 152 (2016) 351–360.
[28] J. Xie, K. Zhang, J. Wu, G. Ren, H. Chen, J. Xua, Bio-nanocomposite films reinforced with organo-modified layered double hydroxides: preparation, morphology and properties, Appl. Clay Sci. 126 (2016) 72–80.
[29] H. Liu, D. Chaudhary, S.I. Yusa, M. Oadé, Glycerol/starch/Na^{+}-montmorillonite nanocomposites: a XRD, FTIR, DSC and ^{1}H NMR study, Carbohydr. Polym. 83 (2011) 1591–1597.
[30] A.H. Navarchian, K. Majdzadeh-Ardakani, F. Sadeghi, Optimization of mechanical properties of thermoplastic starch/clay nanocomposites, Carbohydr. Polym. 79 (2010) 547–554.
[31] M. Lavorgna, F. Piscitelli, P. Mangiacapra, G.G. Buonocore, Study of the combined effect of both clay and glycerol plasticizer on the properties of chitosan films, Carbohydr. Polym. 82 (2010) 291–298.
[32] C.H.C. Flaker, R.V. Lourenço, A.M.Q.B. Bittante, P.J.A. Sobral, Gelatin-based nanocomposite films: a study on montmorillonite dispersion methods and concentration, J. Food Eng. 167 ((2015) 65–70.
[33] G. Qi, N. Li, X.S. Sun, Y. Shi, D. Wang, Effects of glycerol and nanoclay on physiochemical properties of camelina gum-based films, Carbohydr. Polym. 152 (2016) 747–754.
[34] L.A. Castillo, O.V. López, J. Ghilardi, M.A. Villar, S.E. Barbosa, M.A. García, Thermoplastic starch/talc bionanocomposites. Influence of particle morphology on final properties, Food Hydrocoll. 51 (2015) 432–440.

[35] C.K. Saurabh, S. Gupta, J. Bahadur, S. Mazumder, P.S. Variyar, A. Sharma, Mechanical and barrier properties of guar gum based nanocomposite films, Carbohydr. Polym. 124 (2015) 77–84.
[36] M. Huskic, M. Zigon, M. Ivankovic, Comparison of the properties of clay polymer nanocomposites prepared by montmorillonite modified by silane and by quaternary ammonium salts, Appl. Clay Sci. 85 (2013) 109–115.
[37] K.J. Shah, A.D. Shukla, D.O. Shah, T. Imae, Effect of organic modifiers on dispersion of organoclay in polymer nanocomposites to improve mechanical properties, Polymer 97 (2016) 525532.
[38] F. Chivrac, E. Pollet, P. Dole, L. Avérous, Starch-based nanobiocomposites: plasticizer impact on the montmorillonite exfoliation process, Carbohydr. Polym. 79 (2010) 941–947.
[39] B. Saberi, S. Chockchaisawasdee, J.B. Golding, C.J. Scarlett, C.E. Stathopoulos, Development of biocomposite films incorporated with different amounts of shellac, emulsifier, and surfactant, Food Hydrocoll. 72 (2017) 174–184.
[40] J.H. Chen, M.C. Yang, Preparation and characterization of nanocomposite of maleated poly(butylene adipate-co-terephthalate) with organoclay, Mater. Sci. Eng. C 46 (2015) 301–308.
[41] R. Crétois, N. Follain, E. Dargent, J. Soulestin, S. Bourbigot, S. Marais, L. Lebrun, Microstructure and barrier properties of PHBV/organoclays bionanocomposites, J. Membr. Sci. 467 (2014) 56–66.
[42] A. Farahnaky, S.M.M. Dadfar, M. Shahbazi, Physical and mechanical properties of gelatin–clay nanocomposite, J. Food Eng. 122 (2014) 78–83.
[43] B. Tan, N.L. Thomas, A review of the water barrier properties of polymer/clay and polymer/graphene nanocomposites, J. Membr. Sci. 514 (2016) 595–612.
[44] F. Tezcan, E. Gunister, G. Ozen, F.B. Erim, Biocomposite films based on alginate and organically modified clay, Int. J. Biol. Macromol. 50 (2012) 1165–1168.
[45] M. Alboofetileh, M. Rezaei, H. Hosseini, M. Abdollahi, Effect of montmorillonite clay and biopolymer concentration on the physical and mechanical properties of alginate nanocomposite films, J. Food Eng. 117 (2013) 26–33.
[46] C.M.O. Muller, J.B. Laurindo, F. Yamashita, Effect of nanoclay incorporation method on mechanical and water vapor barrier properties of starch-based films, Ind. Crop. Prod. 33 (2011) 605–610.
[47] Y. Chung, S. Ansari, L. Estevez, S. Hayrapetyan, E.P. Giannelis, H. Lai, Preparation and properties of biodegradable starch–clay nanocomposites, Carbohydr. Polym. 79 (2010) 391–396.
[48] A. Giannakas, K. Grigoriadi, A. Leontiou, N.M. Barkoula, A. Ladavos, Preparation, characterization, mechanical and barrier properties investigation of chitosan–clay nanocomposites, Carbohydr. Polym. 108 (2014) 103–111.
[49] J.W. Rhim, Effect of clay contents on mechanical and water vapor barrier properties of agar-based nanocomposite films, Carbohydr. Polym. 86 (2011) 691–699.
[50] D.K.M. Matsuda, A.E.G. Verceheze, G.M. Carvalho, F. Yamashita, S. Mali, Baked foams of cassava starch and organically modified nanoclays, Ind. Crop. Prod. 44 (2013) 705–711.